

Where are *Swift* γ -ray bursts beyond the ‘synchrotron deathline’?

V. Savchenko^{1,2★} and A. Neronov^{1,2}

¹*ISDC Data Centre for Astrophysics, Ch. d’Ecogia 16, 1290, Versoix, Switzerland*

²*Geneva Observatory, Ch. des Maillettes 51, 1290, Sauverny, Switzerland*

Accepted 2009 March 6. Received 2009 March 5; in original form 2009 February 16

ABSTRACT

We study time-resolved spectra of the prompt emission of *Swift* γ -ray bursts (GRB). Our goal is to see if previous BATSE claims of the existence of a large amount of spectra with the low-energy photon indices harder than $2/3$ are consistent with *Swift* data. We perform a systematic search of the episodes of the spectral hardening down to the photon indices $\leq 2/3$ in the prompt emission spectra of *Swift* GRBs. We show that the data of the Burst Alert Telescope (BAT) instrument on board of *Swift* are consistent with BATSE data, if one takes into account differences between the two instruments. Much lower statistics of the very hard spectra in *Swift* GRBs are explained by the smaller field of view and narrower energy band of the BAT telescope.

Key words: radiation mechanisms: non-thermal – gamma-rays: bursts – gamma-rays: observations.

1 INTRODUCTION

In spite of the fact that the phenomenon of the γ -ray bursts (GRB) was discovered more than 40 years ago, its origin and basic physical mechanisms of the observed 0.1–100 s long pulses of hard X-ray /soft γ -ray emission remain obscure. A significant progress in understanding of the GRB phenomenon was achieved over the last decade with the discovery of X-ray, optical and radio afterglows of long (duration > 2 s) (Frail et al. 1997; van Paradijs et al. 1997) and short (duration ≤ 2 s) GRBs (Barthelmy et al. 2005; Fox et al. 2005; Gehrels et al. 2005; Hjorth et al. 2005). Localization of long GRBs in star formation regions, where more than 90 per cent of the supernovae occur, indicates that long GRBs may be produced by the death of massive stars in supernova explosions. This is confirmed by the direct observation of appearance of supernovae at the GRB positions (Galama et al. 1998; Stanek et al. 2003).

The mechanism of production of GRBs is constrained not only by the identification of their multiwavelength counterparts but also by the intrinsic properties of the γ -ray emission. Observations of fast, millisecond-scale, variability during the prompt emission phase (Bhat et al. 1992; Walker, Schaefer & Fenimore 2000) point to the presence of a compact ‘central engine’ powering the GRB, which is naturally associated with a stellar mass black hole or a neutron star formed as a result of the gravitational collapse of a massive star at the onset of a supernova explosion. γ -rays can escape from a relatively compact emission region only if the emitting medium moves with a large bulk Lorentz factor $\gamma_b > 100$ (Fenimore, Epstein & Ho 1993; Woods & Loeb 1995).

Although it is clear that the observed emission is produced by relativistically moving plasma ejected by a newly formed black hole or neutron star, the physical mechanism of the γ -ray emission is not well constrained by the available data. One possibility is that this emission is synchrotron emission from electrons accelerated on ‘internal’ shocks formed in collisions of plasma blobs moving with different velocities (Zhang & Mészáros 2004; Piran 2005). Alternatively, prompt γ -ray emission can be produced via inverse Compton scattering of lower energy synchrotron photons originating from the relativistic plasma itself [the so-called synchrotron-self-compton (SSC) model] (Panaitescu & Mészáros 2000; Kumar & McMahon 2008; Piran, Sari & Zou 2009) or of the photons from external ambient radiation fields [external Compton (EC) model] (Shemi 1994; Shaviv & Dar 1995; Lazatti et al. 2000; Dar & De Rújula 2004; Piran et al. 2009).

Recent detections of strong prompt optical emission from several GRBs seem to indicate the presence of a separate lower energy prompt emission component of the GRB emission (Akerlof et al. 1999; Verstrand et al. 2005, 2006; Racusin et al. 2008). A natural interpretation of this observation would be that optical and soft γ -ray emission are produced, respectively, via synchrotron and inverse Compton mechanisms by one and the same population of relativistic electrons, thus favouring the inverse Compton (SSC or EC) scenario for the 0.01–10 MeV band emission. It is, however, possible that optical and γ -ray components of prompt emission are produced by two separate electron populations and/or in different emission regions (Zou, Piran & Sari 2008). A strong test of the inverse Compton model of the prompt γ -ray emission can be given in the nearest future via (non-)detection of the predicted second-order inverse Compton scattering component in the 1–100 GeV energy band by *Fermi/GLAST* and/or ground-based γ -ray telescopes (Racusin et al. 2008; Savchenko, Neronov & Couvoisier 2009).

★E-mail: Volodymyr.Savchenko@unige.ch

The synchrotron and inverse Compton models of the prompt γ -ray emission could be distinguished via a study of the spectral characteristics of the prompt GRB emission. If the prompt emission is optically thin synchrotron emission from the shock-accelerated electrons in a relativistic ‘fireball’, the spectrum of γ -ray emission could not have photon index harder than that of the synchrotron emission from a monoenergetic electron distribution, $\Gamma_{\text{synch,lim}} = 2/3$ (Katz 1994; Tavani 1995). At the same time, the spectrum of inverse Compton emission can be as hard as $\Gamma_{\text{IC,lim}} = 0$ (Baring & Braby 2004). Observation of episodes of hardening of GRB spectra beyond $\Gamma_{\text{synch,lim}}$ would provide a strong argument against the synchrotron model of the prompt emission (see, however, Epstein 1973; Lloyd & Petrosian 2000; Medvedev 2000; Lloyd-Ronning & Petrosian 2002; Baring & Braby 2004 for modifications of the synchrotron model which are able to accommodate photon indices harder than $2/3$).

The time-resolved spectral characteristics of the prompt GRB emission were studied in details by Preece et al. (1998a,b, 2000) and Kaneko et al. (2006) using a set of bright GRBs detected by the BATSE instrument on board of *Compton Gamma-ray Observatory* (CGRO). The study of BATSE GRBs shows that approximately 30 per cent of all the spectra violate the ‘synchrotron deathline’ $\Gamma = 2/3$ (Preece et al. 1998b). This apparently rules out the synchrotron model as a viable model of the prompt γ -ray emission.

In the view of significance of this result, an independent test of the result with a different instrument is important. However, no such independent test was available so far. In fact, the validity of BATSE result was questioned by the non-observation of excessively hard GRB spectra by the High Energy Transient Explorer (HETE) (Barraud et al. 2003). The HETE–BATSE inconsistency could be resolved by observations with higher sensitivity instruments, such as *Swift*.

In what follows, we perform a systematic analysis of the time-resolved spectra of *Swift* GRBs. We show that, contrary to the initial expectations, *Swift* provides only a very limited possibility for testing the BATSE claim of existence of a significant number of GRBs beyond the ‘synchrotron deathline’. The main problem is that a proper reconstruction of the photon index in the GRB prompt emission spectrum requires a measurement of the break, or cut-off energy, which is not possible with *Swift* because of the limited energy range of its Burst Alert Telescope (BAT). Another difficulty lies in the smaller field of view of *Swift*/BAT, compared to BATSE, which leads to a lower rate of detection of sufficiently bright GRBs, for which the quality of reconstruction of spectral parameters in the time-resolved spectra is comparable to that of the samples of BATSE GRB spectra. Taking into account these difficulties, we show that *Swift* results on detections of very hard GRBs with photon indices beyond the ‘synchrotron deathline’ are consistent with the expectations based on the extrapolation of BATSE results to the *Swift* energy band and sensitivity.

This paper is organized as follows. In Section 3, we explore the potential of *Swift* to test the BATSE result on very hard GRB prompt emission spectra. To do this, we simulate the appearance of BATSE GRBs in BAT telescope on board of *Swift*. We find that only partial tests of BATSE result are possible with *Swift*. In Section 4, we precise this statement and formulate a quantitative prediction on the number of GRB spectra beyond the ‘synchrotron deathline’ which is expected in the *Swift* data. Next, in Sections 5–7 we perform a systematic search of the hard prompt emission spectra in *Swift* GRBs. Finally, in Section 8 we discuss the implications of the observation of a limited amount of GRB spectra beyond the ‘synchrotron deathline’ in *Swift* GRB sample.

2 SPECTRA OF PROMPT γ -RAY EMISSION OF *Swift* GRBS

The spectra of prompt emission from GRBs are conventionally modelled with the ‘Band function’ (Band et al. 1993)

$$\frac{dN_\gamma}{dE} = A \begin{cases} \left(\frac{E}{50 \text{ keV}}\right)^\alpha \exp\left[-\frac{(\alpha - \beta)E}{E_{\text{break}}}\right]; & E < E_{\text{break}} \\ \left(\frac{E_{\text{break}}}{50 \text{ keV}}\right)^{\alpha - \beta} \exp(\beta - \alpha) \left(\frac{E}{50 \text{ keV}}\right)^\beta; & E \geq E_{\text{break}}, \end{cases}$$

where E_{break} is the energy of the break in the spectrum, α and β are, respectively, low- and high-energy photon (spectral) indices and A is the normalization constant. The break energy is related in a simple way to the peak energy of the spectral energy distribution of the GRB, $E_{\text{peak}} = (2 + \alpha)E_{\text{break}}/(\alpha - \beta)$.

The BAT telescope on board of *Swift* is not optimized for the measurement of all the parameters of the Band model (E_{break} , α , β). It is sensitive in the energy range 15–150 keV, while for most of the GRBs E_{peak} is above 150 keV. Instead, the BAT instrument seems to be well suited to the study of the low-energy part of the GRB spectrum, in particular to the measurement of the low-energy photon index α , which is the primary subject of our investigation.

The low-energy part of the GRB spectrum is well described by a cut-off power-law function

$$\frac{dN_\gamma}{dE} = A \left(\frac{E}{50 \text{ keV}}\right)^{-\Gamma} \exp\left(-\frac{E}{E_{\text{cut}}}\right). \quad (2.1)$$

The photon index Γ and the cut-off energy E_{cut} of the cut-off power-law model are simply related to the parameters of the Band model,

$$\Gamma = -\alpha; E_{\text{cut}} = \frac{E_{\text{peak}}}{(2 + \alpha)}. \quad (2.2)$$

Taking into account this one-to-one relation between the Band and cut-off power-law models in the *Swift* energy band, we use the cut-off power law, rather than the Band model for fitting the real *Swift* and simulated BATSE prompt GRB spectra in the following sections.

In the cases when the cut-off energy E_{cut} is not constrained by the data (this can be either when $E_{\text{cut}} > 150$ keV or when $E_{\text{cut}} \leq 150$ keV, but the signal statistics at the highest energies are not sufficient for the measurement of E_{cut}), we further simplify the model spectrum and use a simple power-law model

$$\frac{dN_\gamma}{dE} = A \left(\frac{E}{50 \text{ keV}}\right)^{-\Gamma} \quad (2.3)$$

for fitting of the real and simulated prompt emission spectra.

3 HOW WOULD BATSE GRBS LOOK LIKE IN *Swift*/BAT?

Since the BAT instrument is well suited to the study of the low-energy part of the GRB spectrum, the BATSE observation that some 30 per cent of the time-resolved GRB spectra have low-energy spectral indices harder than $\Gamma = 2/3$ (Preece et al. 1998a) should be readily testable with *Swift*. In order to see if this expectation is true, we first try to find out how the time-resolved spectra of BATSE GRBs from the data base collected by Kaneko et al. (2006) would look like if they would be observed by *Swift*.

The BATSE Gamma-Ray Burst catalogue (Kaneko et al. 2006) includes information on the spectral parameters of the time-resolved GRB spectra as well as information about the time interval durations.¹ The entire data base contains ~ 8000 time-resolved spectra

¹ <http://www.batse.msfc.nasa.gov/kaneko/>

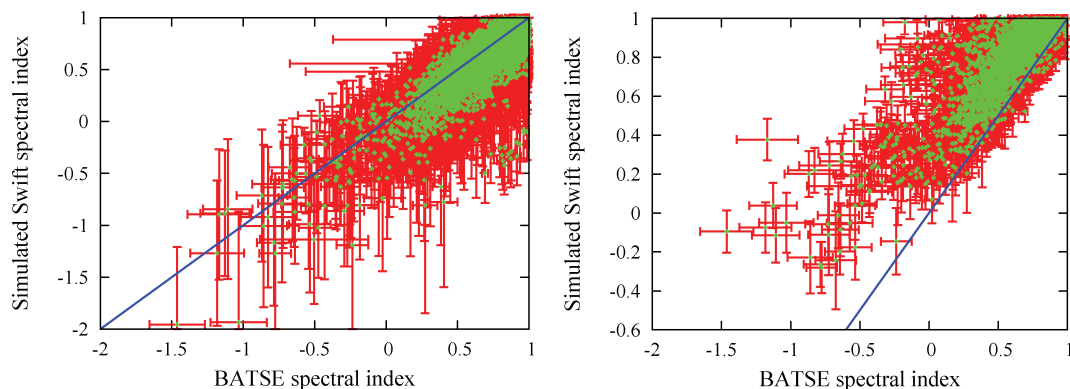


Figure 1. Photon indices, found by fitting simulated BATSE spectra with the CUTE50 (left-hand panel) and with the POWER50 (right-hand panel) models of XSPEC versus the model photon indices. The model parameters are taken from the time-resolved BATSE spectra fitted on a cut-off power-law model. Solid line corresponds to the case when the reconstructed photon index is equal to the input model photon index.

from ~ 300 GRBs detected during ~ 10 years of operation of *CGRO* mission. To simulate the appearance of BATSE GRBs in *Swift*/BAT, we first extrapolate the reported GRB spectra to the BAT energy band (15–150 keV) and then simulate the BAT spectrum, using the XSPEC command `FAKEIT`. We use the `BATPHASIMERR` tool to calculate errors of the simulated spectra, as it is as described in the BAT analysis manual.² In our simulations, we have found that the simulation procedure, described in the BAT analysis manual, does not take into account systematic errors, which are applied in normal data reduction procedure separately, using the `BATPHASYERR` tool. Taking this into account, we separately add a systematic error to the simulated spectra, using `BATPHASYERR` command. In principle, systematic errors, added by the `BATPHASYERR` command, appear to depend on the observation date. We set all simulated spectra at a fake date, the date of GRB 060614.

The BAT telescope on board of *Swift* is a coded mask instrument. The sensitivity of a coded mask instrument is flat throughout the so-called ‘fully coded’ field of view (part of the field of view in which a source illuminates the entire detector), while it degrades in the partially coded part of the field of view (a part in which a source illuminates only a part of the detector). In our simulations, we assume that the GRB always appears in the fully coded field of view. In principle, in a realistic situation it is not true, especially at the initial stage of the GRB, when the BAT first triggers on a burst in a partially coded field of view and then slews towards the direction of the GRB. We discuss the implications of the neglect of the effects of the partially coded field of view in more details in the following sections.

The results of simulations of BATSE GRBs are presented in Fig. 1. From this figure, one can derive several important implications for the search of the hard GRB spectra with *Swift*/BAT telescope.

(i) The error bars of the spectral indices of the simulated BAT spectra are larger than those of the initial BATSE spectra, if both BAT and BATSE spectra are fit on one and the same model, the cut-off power-law model (see left-hand panel of Fig. 1). This is explained by the fact that, in spite of the comparable signal statistics in the original and simulated spectra, the derivation of the errors of the measured spectral indices is affected by the uncertainty of the

measurement of the cut-off energy E_{cut} in the BAT spectrum. This is explained by the limited energy range of BAT detector.

(ii) Taking into account the uncertainty of E_{cut} , we have fitted the simulated spectra on the simple power-law model. This, obviously, reduces the error of the measurement of the photon index, making it comparable to that of the initial BATSE spectra (right-hand panel of Fig. 1). However, ignoring the presence of the cut-off in the spectra results in a systematically softer reconstructed photon index in the simulated spectra. This significantly reduces the number of the very hard spectra, as compared to the original BATSE sample.

Simulations of the time-resolved GRB spectra enable us to estimate the expected amount of hard spectra in the *Swift* GRB sample.

The amount of GRB spectra with the photon indices harder than $2/3$ depends not only on the assumed initial distribution of the photon indices but also on the size of the errors of the reconstructed photon index. The problem is that the statistical scatter of the measurement of the photon index can result in shifts of the values of reconstructed indices towards harder or softer values, thus increasing or decreasing the number of spectra with indices harder than $2/3$. In order to account for this effect, we have performed Monte Carlo simulations, randomly changing the values of the reconstructed photon indices within the errors and assuming Gaussian probability distribution. We have generated histograms of distributions of the photon indices of the ‘randomized’ data sets, similar to that shown in Fig. 2 for the case of the initial simulated BATSE data set. This has enabled us to estimate the typical statistical scatter of the number of GRB spectra in each bin of the histogram. The statistical errors of the numbers of GRBs with given photon indices, computed in this way, are shown in Fig. 2. The uncertainty of the number of GRB spectra with photon indices harder than $2/3$ is also given in the fourth column of Table 1.

As one can see from Table 1, the limited energy range of *Swift* makes the straightforward confirmation/disproval of BATSE result impossible. Even if one would be able to collect a sample of the GRB spectra comparable to that of the BATSE spectral data base, the large uncertainties in the measurement of the photon index within the CUTE50 model would not allow to claim the presence/absence of the GRB spectra with indices harder than $2/3$ at more than 3σ level (see fifth column of Table 1). A better constraint would be, in principle, possible if the spectra are fit on the POWER50 model, in which the uncertainty of the measurement of the photon index

² <http://heasarc.nasa.gov/docs/swift/analysis/threads/batsimspectrumthread.html>

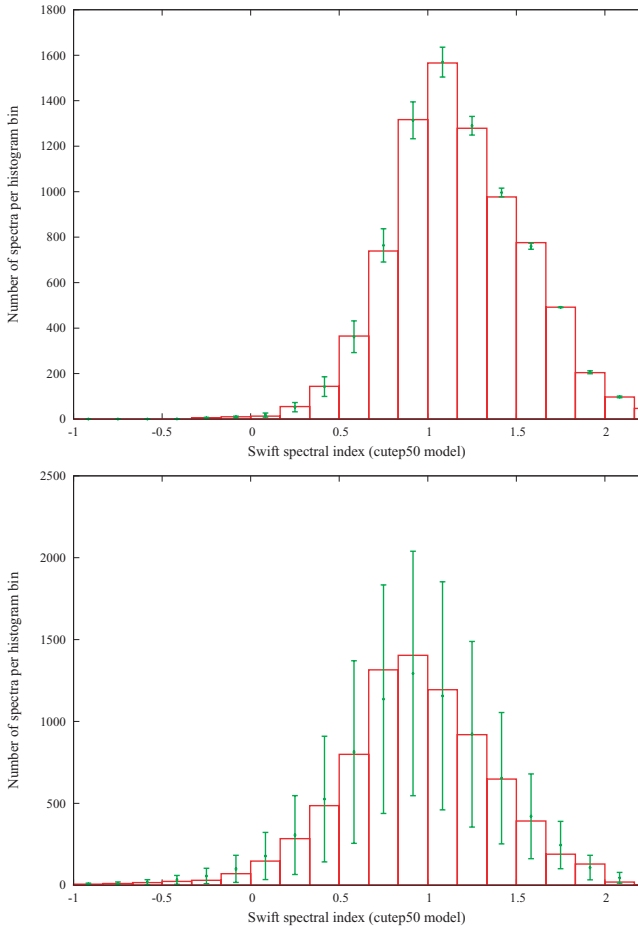


Figure 2. Upper panel: histogram of the reconstructed low-energy power-law indices (fit on the POWER50 model) of simulated BATSE GRB spectra. Lower panel: same, but for the fit on the CUTEP50 model of xspec.

is somewhat lower. In this case, a clear confirmation/disproval of BATSE result at 6σ level would be possible with a sample of the size comparable to that of the BATSE spectral data base.

However, the sample of *Swift* GRBs chosen using the selection criteria similar to those used in the BATSE data base results in a sample which is ~ 20 times smaller than the complete BATSE sample. Indeed, BATSE was an all-sky monitor, while the (partially

+ fully coded) field of view of BAT is limited to 1.4 sr (Gehlers et al. 2004), which is $4\pi/1.4 \simeq 10$ times smaller than that of BATSE. Besides, BATSE telescope operated over the 10-year time period, while the BAT has only been four years in orbit. Adopting *exactly* identical selection criteria for *Swift* GRBs would, therefore, result in selection of $8 \times 10^3 \cdot 0.1 \cdot (4/10) \simeq 3 \times 10^2$ time intervals. Rescaling our simulation results to a smaller sample of GRB spectra (see rows 3 and 4 in Table 1), one finds that the number of GRB spectra with reconstructed photon indices harder than 2/3 is dominated by the statistical uncertainty, so that no definite conclusion can be drawn about presence/absence of such hard spectra, based on the analysis of the histogram of distribution of the photon indices.

4 METHOD OF TESTING THE BATSE RESULT

The large statistical uncertainty of the number of reconstructed GRB spectra with photon indices harder than 2/3 leaves only a limited possibility to test the presence of the very hard spectra during the prompt emission phase with *Swift*. This possibility is related to the fact that in the BATSE GRB spectra sample there exist a certain amount of bursts for which the measured spectra are characterized by low-energy photon indices harder than 2/3 at $\geq 3\sigma$ confidence level. One expects to find similar high-confidence hard spectra in a subset of the time-resolved *Swift* GRB spectra. Comparing the number of detected hard GRB spectra with that expected from the simulations of the BATSE GRB spectral sample, one can readily test BATSE result. Contrary to the method based on the analysis of the distribution of the low-energy photon indices, discussed above, such a ‘direct’ method does not suffer from the statistical uncertainties of the distribution of the photon indices.

A potential problem of the proposed method is that the episodes of extreme hardening of the spectra are not randomly distributed over the BATSE GRB sample. In fact, the episodes of hardening last for more than one time bin, so that individual GRBs in which the hard indices are found, possess multiple time intervals with hard spectra. This is clear from the last column in Table 1. One can see that in spite of the considerable amount of time intervals with hard spectra (28 in the case of CUTEP50 model) expected in *Swift* GRB sample, these intervals are expected to be found in only ~ 5 GRBs. This means that the GRBs with hard photon indices are extremely rare events for *Swift*. One expects to find ~ 1 such event per year. The expectation is still worse, if one adopts the POWER50 model for the spectral analysis. In this case, one expects to detect one such

Table 1. Statistics of GRB spectral parameters in different samples. Top two rows show the data for the simulations of BATSE GRBs from the sample of Kaneko et al. (2006) assuming BAT response. The sample marked as ‘BATSE, scaled (1)’ is the rescaling of the full sample of simulated BATSE spectra, taking into account smaller exposure of *Swift*. The sample marked as ‘BATSE, scaled (2)’ is a rescaling of the full simulated BATSE sample for the smaller number of *Swift* GRBs, with additional assumption that the error of the reconstructed photon index is two times larger than that implied via the simulation procedure discussed in the text. Last two rows show the statistics of the spectral parameters for the sample of real *Swift* GRBs selected following the criteria given in Section 5.

Data sample	Spectral model	Total number of indices	Indices smaller than 2/3	Significance	Indices harder than 2/3 at $\geq 3\sigma$ level
BATSE	CUTEP50	8072	2080 ± 611	3.4	809 in 138 GRBs
BATSE	POWER50	8129	607 ± 101	6.0	342 in 66 GRBs
BATSE, scaled (1)	CUTEP50	278	71 ± 113		28 in 5 GRBs
BATSE, scaled (1)	POWER50	300	22 ± 19		13 in 2.4 GRBs
BATSE, scaled(2)	CUTEP50	278	81 ± 190		2 in 1
BATSE, scaled(2)	POWER50	300	24 ± 40		3.4 in 1
BAT	CUTEP50	343	19 ± 8	2.4	4 in 2 GRBs
BAT	POWER50	367	7 ± 3	2.3	0 in 0 GRBs

event per 2 years on average. In the following section, we report the results of a systematic search of the episodes of hardening of spectra beyond $\Gamma = 2/3$ in the real data of BAT telescope on board of *Swift*.

5 SELECTION OF *Swift* GRBS FOR THE TIME-RESOLVED SPECTRAL ANALYSIS

The BATSE sample of the time-resolved GRB spectra which we have used for our simulations in the previous section was selected from sufficiently bright bursts detected over a 10-year span of the *CGRO* mission according to the selection criteria (Kaneko et al. 2006):

(A) energy fluence in 20–2000 keV energy band is larger than $2 \times 10^{-5} \text{ erg cm}^{-2}$ or

(B) peak flux in a 256 ms time bin is higher than 10 photons $\text{cm}^{-2} \text{ s}^{-1}$ in 50–300 keV energy band.

Each of the selected BATSE GRBs was binned in time intervals for the time-resolved spectral analysis, according to the following principle:

(C) signal-to-noise ratio (S/N) in the time interval is ≥ 45 .

Obviously, because of the difference in the *Swift*/BAT and BATSE energy bands, it is not possible to literally adopt the same selection criteria (A) and (B) for selection of *Swift* GRBs. However, it is straightforward to work out a selection criteria for the time intervals, equivalent to (C), using the sample of simulated BATSE GRBs. The upper panel of Fig. 3 shows the distribution of S/Ns [expressed in the ‘total counts’, i.e. $(S/N)^2$ plotted over x -axis] for the simulated BATSE GRB spectra, together with the durations of the time intervals and errors of the measurement of the photon indices (adopting model *POWER50*). One can see that the time binning which corresponds to $S/N=45$ in BATSE is equivalent to a similar $S/N \sim 30$ –40 or to the photon statistics $\sim 10^3$ in *Swift*.

To select the time intervals with $S/N \sim 30$ –40 from the real *Swift* data, we adopt the following procedure. The BAT light curves are usually presented in terms of the ‘normalized counts’, which are the photon counts which would be detected from an equivalent on-axis source, rather than from the real GRB source at non-zero off-axis angle. Selection of the time intervals for the spectral analysis in

terms of the photon statistics estimated from the ‘normalized counts’ usually overestimates the S/N, because (i) the burst could initially occur in the partially coded field of view and (ii) the ‘normalized counts’ statistics do not take into account the systematic error of the photon flux measurement. Having this in mind, we have found that reformulating the time binning principle as

(C1) S/N in the time interval for spectral extraction is ≥ 60

results in a distribution of the errors of measurement of the photon indices in the real *Swift* data, which are similar to those of the simulated BATSE spectra. This is demonstrated in the lower panel of Fig. 3 where the S/Ns, errors of the measurement of the power-law index and durations of the time intervals selected in the real *Swift* GRB spectra are shown. Comparing the lower and upper panels of Fig. 3, one finds that the main difference between the simulated BATSE and real *Swift* spectra selected according to the above criteria (C) and (C1), respectively, is in the duration of the time intervals. Somewhat longer durations of the time intervals in the real *Swift* data are explained by the fact that in our simulations of BATSE spectra we have ignored the possibility that the GRB can occur at large off-axis angle and/or because the simulation procedure occasionally underestimates the systematic measurement errors.

Imposing a simple selection criterion on the GRBs that

(AB1) GRB contains at least one time interval suitable for spectral extraction,

we have selected a set of 80 *Swift* GRBs, listed in Table 2. Binning the selected GRBs on to time intervals for the spectral extraction, we have obtained $\sim 3 \times 10^2$ time-resolved spectra (see Table 1). As expected, the overall size of the *Swift* GRB spectral sample is some ~ 20 times smaller than that of the BATSE spectral data base.

The selection criterion (AB1) adopted for *Swift* GRBs is weaker than the criteria (A,B) used for the selection of BATSE GRBs. This means that, in principle, one should select more GRBs for the spectral analysis, than expected from the simple rescaling of the BATSE GRB sample. An overestimate of the expected number of *Swift* GRBs satisfying the selection criteria of BATSE GRBs, found in the previous section, is related to the fact that we have ignored the decrease of the telescope sensitivity in the partially coded field of view. However, based on the estimates of the previous section, one can see that already with the relaxed selection criterion (AB1), which reduces the amount of the time intervals available for the spectral analysis down to ~ 300 , one is left with a very limited possibility to test the BATSE result on the existence of very hard GRB spectra. Taking this into account, we limit our selection criteria to (AB1) and adopt the requirement (C1) for the choice of time binning of the selected GRBs.

Relaxing the criteria for the GRB selection, in fact, changes the GRB sample under consideration. To illustrate this fact, we plot in Fig. 4 the distribution of the overall fluences of the selected *Swift* GRBs, as compared to that of the BATSE GRBs used for the spectral analysis by Kaneko et al. (2006). One can see that by relaxing the selection criteria we add a large amount of bursts with low fluences. Another important difference is that the time binning of the additional lower fluence GRBs is characterized by longer typical integration times of the spectra (shown by the magenta dotted line in Fig. 4). The presence of an additional population of weaker GRBs in the sample is not a problem for the method described in Section 4: one looks for episodes of high-confidence-level spectral hardening in several individual bursts rather than study statistical properties of the entire selected GRB sample.

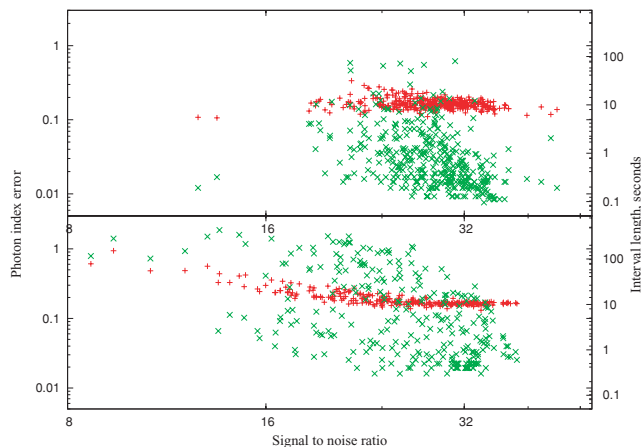
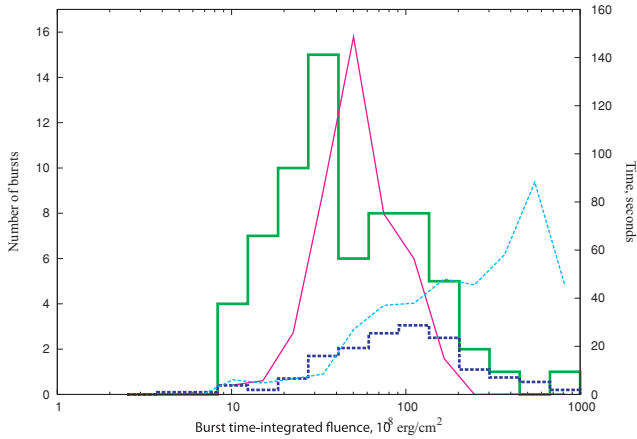


Figure 3. Errors of measurement of the photon index (red/dark grey) and the durations of the time intervals selected for the spectral extraction (green/light grey points) as functions of the S/Ns. The upper panel shows the simulated BATSE spectra. The lower panel shows the real *Swift* data.

Table 2. *Swift* GRBs selected for the analysis.

Name	Fluence	<i>N</i>	Name	Fluence	<i>N</i>	Name	Fluence	<i>N</i>	Name	Fluence	<i>N</i>
GRB 041223	163	7	GRB 041224	54.9	1	GRB 050117	65.3	2	GRB 050219B	95.3	1
GRB 050306	111	1	GRB 050418	41	1	GRB 050525A	152	20	GRB 050713A	28.3	1
GRB 050717	53.5	2	GRB 050724	11.2	1	GRB 050820B	16.1	2	GRB 050904	45.3	1
GRB 050915B	34	2	GRB 050922C	15.7	1	GRB 051111	25.6	1	GRB 051117A	31.6	1
GRB 051221A	9.29	1	GRB 060105	134	5	GRB 060117	161	7	GRB 060210	60	1
GRB 060322	33.8	1	GRB 060413	21.1	1	GRB 060418	67.7	2	GRB 060510B	27.9	1
GRB 060607A	22.6	1	GRB 060614	198	16	GRB 060729	27	1	GRB 060813	16.9	1
GRB 060929	5.31	1	GRB 061007	425	31	GRB 061021	14.6	1	GRB 061121	125	17
GRB 061126	24.5	1	GRB 061202	24.6	2	GRB 061222A	68.4	6	GRB 070107	41.4	1
GRB 070129	20.4	1	GRB 070220	86.1	4	GRB 070306	28	2	GRB 070328	17.9	1
GRB 070419B	69.3	3	GRB 070420	118	1	GRB 070521	76.9	4	GRB 070612A	97.5	1
GRB 070616	181	8	GRB 070621	44.9	1	GRB 070721B	28.5	1	GRB 070911	104	7
GRB 070917	9.82	1	GRB 071003	35.5	1	GRB 071010B	19.7	3	GRB 071020	17.3	2
GRB 071117	15	1	GRB 080207	30.4	1	GRB 080229A	71	3	GRB 080310	18.6	1
GRB 080319B	772	96	GRB 080328	79.5	3	GRB 080411	253	31	GRB 080413A	32	2
GRB 080413B	25.9	1	GRB 080503	19.3	1	GRB 080603B	12	1	GRB 080605	123	6
GRB 080607	222	4	GRB 080613B	37.5	2	GRB 080810	33.1	1	GRB 080916A	33.1	2
GRB 080928	18.4	1	GRB 081008	29.6	1	GRB 081028A	32.2	1			

**Figure 4.** Distribution of the GRB fluences. Green thick solid line: *Swift* GRB fluences; blue dashed thick line: BATSE GRBs in *Swift* BAT (number of events rescaled to *Swift* effective exposure). Thin solid line – median duration of the bursts included in current bin in the *Swift* data, thin dashed line: durations of the bursts in the simulated BATSE GRB sample.

6 DATA REDUCTION AND ANALYSIS

To analyse the set of selected *Swift* GRBs in a homogeneous way, we have developed a pipeline script (which is similar to BATGRBPRODUCT pipeline script provided by the *Swift* team). We use HEASOFT-6.5.1 and latest calibration data base in our analysis.

Using BAT science analysis tasks BATMASKWTEVT (applying detector mask corrections from auxiliary files and estimated by detector plain image hot pixels) and BATBINEVT, we produce ‘mask-tagged’ light curves for each burst selected and for different time binning (we select time binning intervals as 5, 100, 500 and 2000 msec for each burst). Auxiliary *Swift* slew information extracted during mask weighting is saved for further use. The light curves are built in units of background-subtracted counts per fully illuminated detector for an equivalent on-axis source, or ‘normalized counts’, as it is defined in the *Swift* User Guide. Overall time intervals of the burst light curves considered in our analysis were selected with the help

of BATTBLOCKS tool τ_{99} (time interval containing 99 per cent of GRB fluence). We knowingly choose too long time around real GRB and reject remaining background intervals (identified as intervals with low peak flux) after analysis.

At the next stage of analysis, the GRB light curves are rebinned to achieve the required S/N, given by the selection criterion (C1) (see Section 4). The significance of the signal detection normally cannot be extracted directly from the information about the ‘normalized counts’ found in the light curves. This is related to the fact that the flux measurement error can be determined only after background subtraction via mask-weighting technique and by taking into account the systematic errors. In order to characterize the significance of the signal detection, we introduce the ‘real counts’ in each time bin via the relation $C_{\text{real}} = (F/\Delta F)^2$, where F is the flux and ΔF is the flux measurement error. Each time bin selected for the spectral analysis is required to accumulate the number of real counts above a certain threshold. We perform the analysis via several parallel pipelines, which differ by the choice of the required number of real counts per time bin. Choosing the binning with a relatively small number of real counts, 100, 400 and 900 per time bin, we are able to trace the spectral evolution of the bursts on shorter time-scales. On the other side, choosing a large number of real counts per time bin enables us to obtain higher quality spectra.

The choice of 4000 real counts per bin (criterion C1 for the GRB time binning) results in the quality of reconstruction of spectral parameters from the BAT spectra, which is comparable to that found in the simulated BATSE spectra. This is illustrated in the lower panel of Fig. 3, where the errors of measurement of the photon index as a function of significance of detection are shown. One could note that the significance of the signal detection found from the BAT spectrum (plotted along the x -axis in Fig. 3) is systematically lower than that found from the BAT light curve (assumed to be constant in all time bins, $\sim\sqrt{4000} \simeq 63$). This is related to the fact that the *Swift* spectral and light curve extraction procedures use different estimates of systematic errors.

Having binned the GRB in time intervals with sufficient S/N, we perform spectral extraction procedure in each time bin. The entire 15–150 keV energy interval is divided on to 10 energy bins: 15–25, 25–35, 35–45, 45–55, 55–65, 65–75, 75–90, 90–105, 105–125

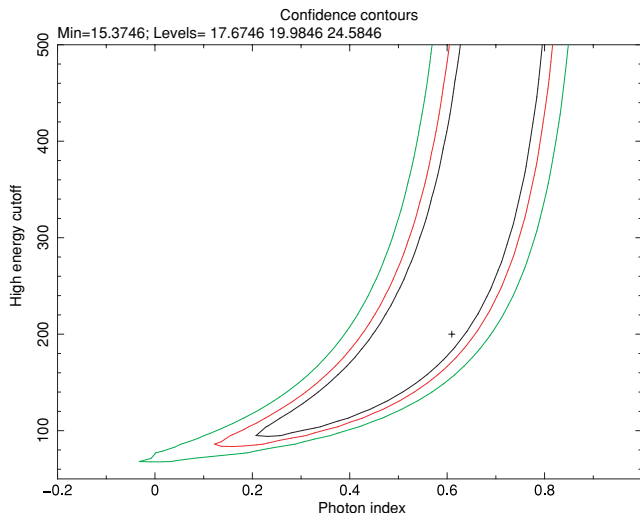


Figure 5. Chi-squared levels for fitting a typical BAT spectrum with cut-off power-law model. *Swift* GRB spectra, fitted on the CUTE50 model.

and 125–150 keV. The spectra are extracted with the help of the BATBINEVT tool. The response matrices are produced with the help of the BATDRMGEN tool. We insert the proper ray-tracing keywords into the DRM file with the help of BATUPDATEPHAKW. The systematic error vector is produced with the help of BATPHASYERR and applied to the spectrum.³

The individual spectra are analysed with the help of XSPEC package.⁴ The spectral fits are done using both POWER50 (power law normalized at 50 keV) model and cut-off power-law CUTE50 (power law with high-energy cut-off, normalized at 50 keV) model of XSPEC, recommended by the BAT team.⁵ As discussed above, in the energy range covered by *Swift*, the phenomenological Band model for the spectrum (2.1) is equivalent to the cut-off power-law CUTE50, with the photon index and cut-off energy simply related to the low-energy photon index α and the break energy E_{break} of the Band model (see equation 2.2).

The cut-off energy E_{cut} is higher than 150 keV for a large fraction of GRBs. This means that this energy cannot be fully constrained by *Swift*/BAT. Taking this into account, we fit the spectra with two alternative models: CUTE50 and POWER50, the latter being appropriate when E_{cut} lies much above the BAT energy band.

It is clear that fitting the spectra with a cut-off power-law model results in a larger uncertainty of the measurement of the photon index, because of a parameter degeneracy arising in simultaneous measurement of the photon spectra index and the cut-off energy. This effect is illustrated in Fig. 5 where we show 1σ – 3σ error contours in the E_{cut} , Γ plane for a typical GRB spectrum. One can see that although the cut-off energy is not constrained by the fit, it affects the error of the photon index, effectively increasing it by a factor of 2. The uncertainty of calculation of the photon index is much smaller in the fits on the power-law model, where the parameter E_{cut} is absent.

³ see for details http://swift.gsfc.nasa.gov/docs/swift/analysis/bat_digest.html.

⁴ XSPEC reference.

⁵ <http://heasarc.gsfc.nasa.gov/docs/swift/analysis/threads/batspectrumthread.html>

7 *Swift* GRBS BEYOND THE ‘SYNCHROTRON DEATHLINE’

7.1 Spectral evolution of individual *Swift* bursts

The entire set of *Swift* GRBs selected according to the criterion (AB1) and time binned following the criterion (C1) (see Section 3) reveals that only two GRBs in which in total five time intervals with hardening of the spectrum down to the photon indices $\Gamma < 2/3$ at $\geq 3\sigma$ level are observed. These are GRB 061007 and GRB 080319B. The light curves of these GRBs and the evolution of the photon index over the burst duration are shown in Fig. 6.

7.2 GRB 080319B

GRB 080319B is the GRB with the highest fluence in the *Swift* GRB sample (see Table 2). The period of spectral hardening beyond $\Gamma = 2/3$ occurs during the first 10 s of the burst duration (see Fig. 6a). GRB 080319B is one of the few GRBs for which a bright prompt optical emission was detected (Racusin et al. 2008). The optical emission flux is above the power-law extrapolation of the observed γ -ray flux. This indicates that the optical emission forms a separate component which is either produced by a separate population of relativistic electrons or, otherwise, produced by the same population of electrons, but via a different physical mechanism. It is interesting to note that the moment of onset of the flash coincides with the moment of softening of the spectrum from $\Gamma \leq 2/3$ down to $\Gamma \simeq 1$ (see Fig. 6a). This gives a clue to the understanding of the mechanism of the strong optical emission (Savchenko et al. 2009) and, possibly, for the understanding of the mechanism of production of very hard γ -ray emission spectrum during the first 10 s of the burst.

7.3 GRB 061007

GRB 061007 is the GRB with the second highest fluence in the *Swift* GRB sample. It is remarkable that the episodes of spectral hardening down to the photon index $\Gamma \leq 2/3$ are detected in the two brightest GRBs. This is consistent with our conclusion that the sensitivity of BAT telescope is only marginally sufficient for the detection of the very hard GRB spectra: the study of the spectral evolution with sufficient time resolution is possible only for the brightest bursts. Contrary to GRB 080319B, the episode of hardening of the spectrum down to $\Gamma \leq 2/3$ in GRB 061007 is observed in the middle, rather than at the beginning of the burst. However, one could note that the episode of the hardening coincides with the start of a pronounced subflare (see Fig. 6b).

7.4 Other GRBs with the episodes of spectral hardening

The fact that only two brightest bursts from our *Swift* GRB sample reveal the episodes of spectral hardening beyond $\Gamma = 2/3$ may indicate that our requirement (C1) adopted for the time binning of the GRB light curve is too restrictive. The typical width of the time bins chosen for the spectral analysis in weaker GRBs turns out to be longer than the typical duration of the episodes of the spectral hardening. It is possible that relaxing the constraint on the overall significance of the signal detection within the time bin one may be able to find more episodes of spectral hardening in the time-resolved GRB spectra.

This expectation is confirmed by our re-analysis of the data with different choice of the time binning, which reveals other GRBs with

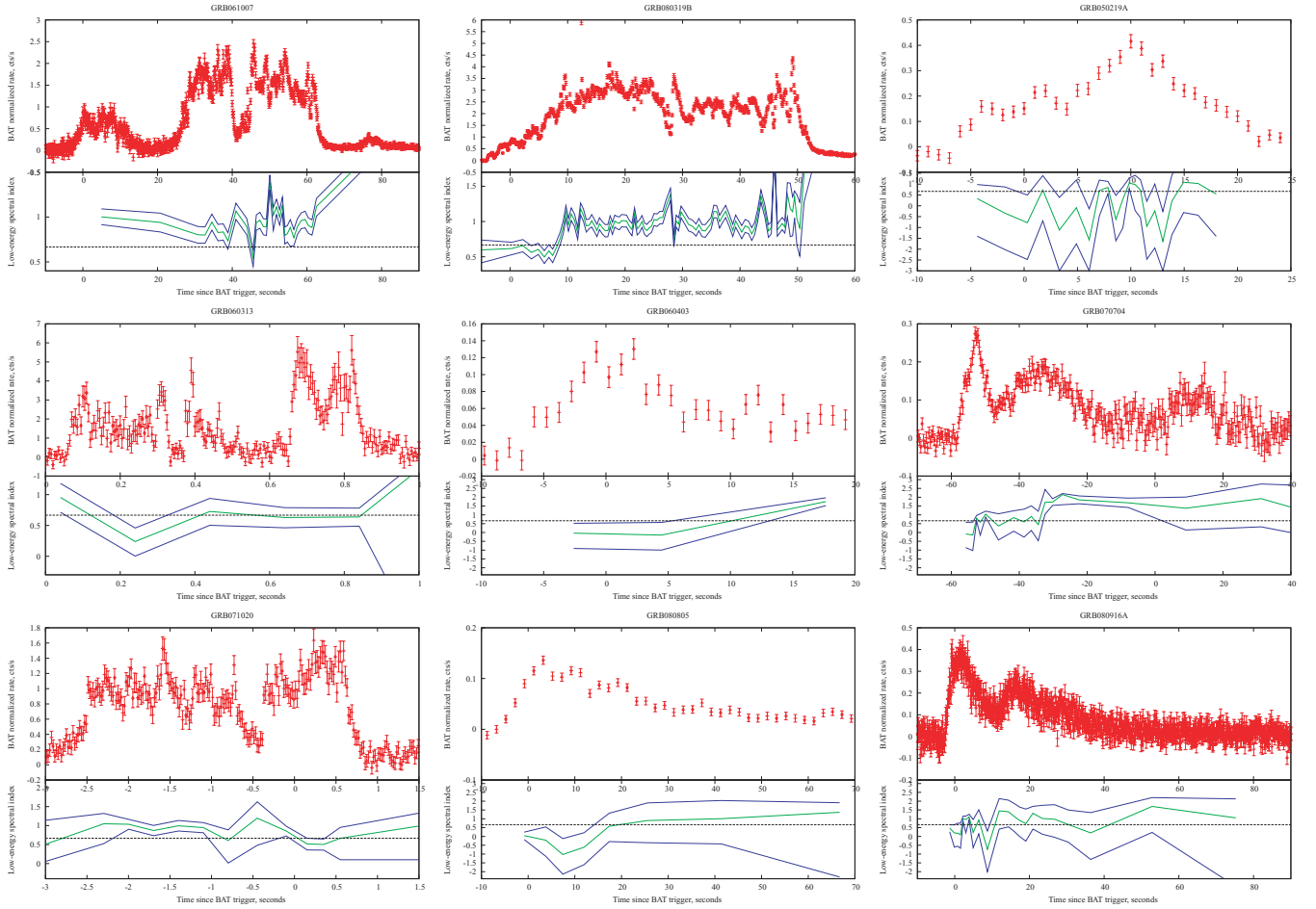


Figure 6. Episodes of spectral hardening beyond $\Gamma = 2/3$ in *Swift* GRBs. Top panels show the 15–150 keV band light curves. Bottom panels show the evolution of the photon index in the *CUTEP50* model (green curves). Blue curves show the 3σ errors of the measurement of the photon index. Horizontal dashed line in the bottom panels shows the limiting photon index of the optically thin synchrotron emission, $\Gamma = 2/3$.

the episodes of spectral hardening, GRB 050219A, GRB 060313, GRB 060403, GRB 070704, GRB 071020, GRB 080805 and GRB 080916A, shown in panels (c)–(i) of Fig. 6.

To the best of our knowledge, not all the above-listed episodes of spectral hardening down to $\Gamma < 2/3$ were previously reported. In the case of GRB 050219A, the spectral hardening is discussed by Goad et al. (2005). GRB 060313 is listed as the hardest of the *Swift* bursts [based on the (50–100)/(25–50) keV ratio] in (Romig et al. 2006).

The episodes of spectral hardening do appear preferentially at the onset of the bursts or of the bright subflares within the bursts. The same effect is observed in the case of BATSE GRBs, where the episodes of harder than $\Gamma = 2/3$ spectra appear preferentially at the beginning of the burst (see Fig. 7).

The appearance of the episodes of spectral hardening preferentially at the onset of the bursts reveals an additional difficulty for detection of such intervals with *Swift*. Namely, a significant fraction of the GRBs is initially detected in the partially coded field of view of the BAT telescope (see Fig 8). In this part of the field of view, the sensitivity of the telescope degrades, which leads to a decrease of the signal statistics. This results in a decrease of the precision of the measurement of spectral parameters. This, in turn, leads to the decrease of efficiency of detection of the episodes of spectral hardening at the onset of the burst. This effect was not included in our simulations of BATSE GRB

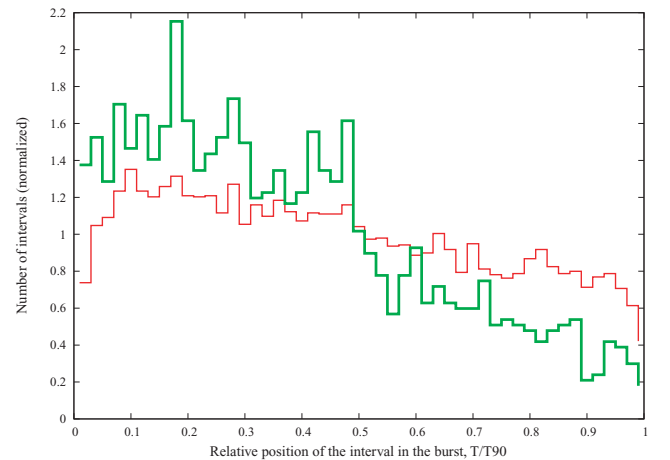


Figure 7. Distribution of the times episodes of hardening of the spectra of BATSE GRBs beyond $\Gamma = 2/3$ over the duration of the GRB (green) compared to the overall distribution of the numbers of time-resolved GRB spectra throughout the GRB duration (red).

spectra. As a result, our prediction of the expected number of GRB spectra harder than $\Gamma = 2/3$ at $\geq 3\sigma$ confidence level, based on the simulations of BATSE spectra, is, in fact, an overestimate.

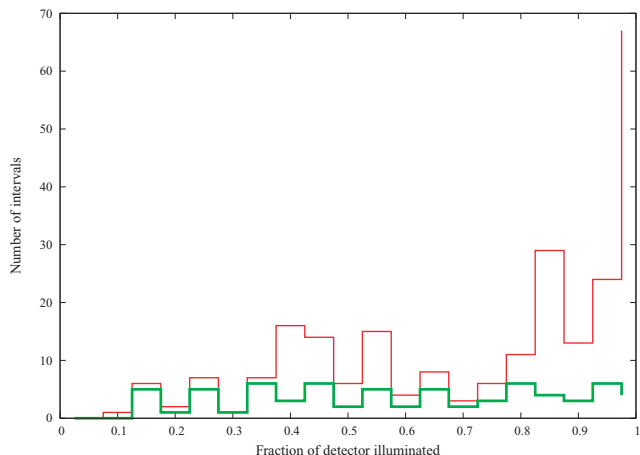


Figure 8. Distribution of the illumination fractions of BAT detector surface

To find out how the underestimate of the error of measurement of the photon index in the simulations of BATSE spectra influences the prediction of the amount of GRB spectra beyond the ‘synchrotron deathline’, we present in Table 1 [simulated GRB sample called ‘BATSE, scaled (2)’] the results of simulation of BATSE GRB spectra with BAT response, assuming that the error of measurement of the photon index is two times larger than that predicted by the our initial simulation algorithm, described in Section 3. One can see that a factor of 2 increase of the measurement error results in a dramatic decrease of the expected detections of the episodes of spectral hardening (~ 2 time intervals in ~ 1 GRB in four years of *Swift* data).

Taking into account this uncertainty on the error of the measurement of the photon indices in the simulations of BATSE GRBs, one can conclude that the detection of five intervals of hardening of the spectra beyond $\Gamma = 2/3$ at $\geq 3\sigma$ confidence level in *Swift* GRB data set is consistent with the expectations derived from the simulations of observational appearance of BATSE GRBs in BAT.

7.5 Distribution of low-energy photon indices in *Swift* GRBs

In this section, we present the distribution of the GRB photon indices derived from the real *Swift* data for the two spectral models (POWER50 and CUTEP50) used in our spectral analysis. As it is mentioned above, we have relaxed the GRB selection criteria for *Swift* GRBs to the single criterion (AB1), compared to the tighter criteria (A) and (B) used for the BATSE GRBs in the sample studied by Kaneko et al. (2006). This has resulted in the inclusion of lower fluence and lower flux GRBs in our sample (see Fig. 4).

The difference in the selection criteria results in a difference in the distribution of spectral parameters in the sample of time-resolved spectra of GRBs in the *Swift* GRB sample. This is illustrated in Fig. 9, where we show the histograms of distributions of the photon indices found in fitting the burst spectra on the cut-off power law and on the simple power-law models. Uncertainties on the numbers of photon indices in each bin of the histograms were computed in the same way in the case of Fig. 2, via Monte Carlo simulations of sets of photon indices in which the photon indices are randomized within the errors of measurements, around the value observed in the real data.

One can see that, as expected, no statistically significant excess of the very hard spectra with indices below $\Gamma = 2/3$ is observed.

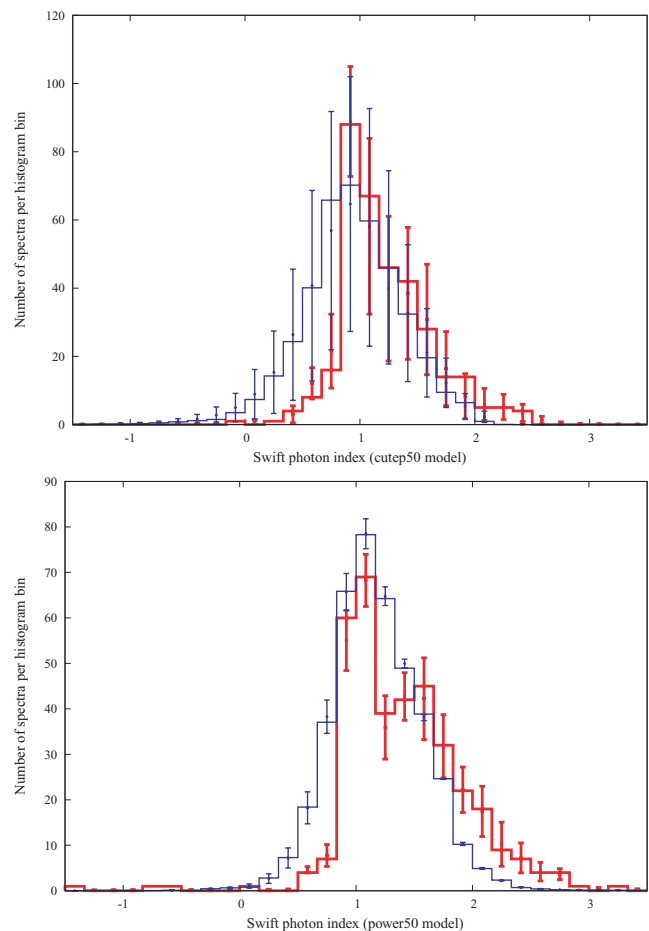


Figure 9. Distribution of photon indices of the time-resolved spectra of *Swift* GRBs (thick red lines). The upper panel shows the results for the CUTEP50 spectral model. The lower panel shows the result for the POWER50 model. For comparison, the distribution of photon indices of the simulated BATSE spectra is shown by the thin blue lines. The distributions of the photon indices of the simulated BATSE spectra are rescaled to be comparable in height to the *Swift* photon index distributions.

The numbers of spectra with photon indices below $2/3$ and their statistical uncertainties are given in the last two rows of Table 1 for the two spectral models used in our analysis.

For comparison, we also show in Fig. 9 the histograms of distributions of the photon indices found from simulations of the BATSE GRB spectra, discussed in Section 3. One can see that slightly different choices of selection criteria for the *Swift* GRBs result in the appearance of larger number of softer time-resolved spectra in *Swift* sample, compared to the BATSE sample. This is readily explained by the fact that in the included weaker GRBs longer integration times are needed to achieve the required S/N. The GRBs typically exhibit the so-called hard-to-soft spectral evolution. This implies that with longer integration time one finds, in general, a softer spectrum.

8 DISCUSSION

The goal of our study of time-resolved spectral of *Swift* GRBs was to clarify if *Swift* is able to confirm or disprove BATSE observation that some ~ 30 per cent of spectra of the prompt emission phase are characterized by very hard low-energy photon indices, $\Gamma < 2/3$ (Preece et al. 1998a). This observation is potentially

important because it rules out the optically thin synchrotron emission model of the prompt emission phase.

The validity of the BATSE result was questioned by non-observation of the excessively hard GRB spectra with HETE (Barraud et al. 2003). It was expected that an independent test of validity of BATSE result will become available with the help of *Swift*, which is sensitive in the energy range 15–150 keV, optimal for the precision measurement of the low-energy spectral indices of the GRB prompt emission phase (Baring & Braby 2004).

Our study shows that

(i) it is not possible to fully test the BATSE claim of existence of too hard GRB spectra ‘beyond the synchrotron deathline’ with *Swift* and

(ii) the statistics of the spectral parameters of *Swift* GRBs are consistent with the assumption of existence of a significant fraction of prompt emission spectra beyond the ‘synchrotron deathline’.

Contrary to the initial expectations, the constraints on the low-energy photon indices found from the *Swift* data are much weaker than those found from the BATSE data. This is explained by several differences between BATSE telescope on board of *CGRO* and BAT instrument on board of *Swift*.

The limited energy range of BAT instrument (sensitive at the energies up to 150 keV) precludes a measurement of the cut-off or break energies in a large fraction of time-resolved GRB spectra. The uncertainty in the cut-off energy introduces a large uncertainty in the measurement of the photon index, if the GRB spectra are fit with a cut-off power-law model (CUTEP50). This effect is illustrated in Fig. 5, showing the error contours in the $E_{\text{cut}} - \Gamma$ parameter space for a typical GRB spectrum from a *Swift* GRB sample. Larger measurement errors affect the distribution of photon indices of the time-resolved GRB spectra. This leads to ‘washing out’ of the statistically significant hard tail in the distribution of the photon indices. This is demonstrated in the fourth column of Table 1, where the statistics of the GRB spectra with the photon indices harder than $2/3$ are shown. One can see that even if the size of the sample of the time-resolved GRB spectra in *Swift* would be comparable to that of the samples of BATSE time-resolved spectra ($\sim 8 \times 10^3$ spectra), it would not be possible to test the existence of the harder than $\Gamma = 2/3$ spectra with the *Swift* data, if the cut-off power-law model (CUTEP50) would be used for the spectral fitting.

One can see from Table 1 that if the size of the *Swift* GRB spectral sample would be comparable to that of BATSE, a statistical test of the BATSE result on the hard GRB spectra would still be possible if the data are fit with the simple power-law model (POWER50) without the high-energy cut-off. Spectral fitting in this model does not suffer from the uncertainty related to the uncertainty of measurement of the cut-off energy, mentioned above. This leads to tighter constraints on the measurement of the photon index.

However, a 10 times smaller field of view and shorter operation time of *Swift* explain the much smaller size of the sample of the time-resolved GRB spectra, compared to the BATSE spectra sample. We have been able to generate some ~ 300 time-resolved GRB spectra, using a selection criterion, similar to that used in the BATSE time-resolved spectral analysis (sufficient S/N within a given time interval). This amount is more than a factor of 20 smaller than the number of time-resolved spectra in the BATSE data base. Lower statistics of the GRB spectral sample further reduce the possibility to test the BATSE result, even if the power-law model is used for the spectral fitting. As one can see from Table 1, the expected statistical uncertainty of the numbers of GRB spectra with given photon indices is too large, so that the spectra with $\Gamma < 2/3$ still

can be easily confused with the statistical scatter of the spectra with $\Gamma > 2/3$ within the measurement errors.

Having analysed the limitations of the BAT instrument via simulations of the observational appearance of BATSE GRBs in the BAT detector, we have found that the only available possibility to test the BATSE result with *Swift* data is to systematically search for the episodes of spectral hardening beyond $\Gamma = 2/3$ in the entire *Swift* GRB sample. The idea was to find (or constrain the amount of) the time intervals with relatively high flux and hard spectrum, so that the errors of measurement of the photon index are small enough and the measured photon index is harder than $\Gamma = 2/3$ at $\geq 3\sigma$ confidence level. If found, the photon indices such ‘high-confidence’ hard spectra cannot be confused with the softer photon indices which occasionally could appear to look harder because of the scatter within the measurement error. An estimate of the expected number of GRBs with such ‘high-confidence’ hard spectra in *Swift* shows that some two to five GRBs with sufficiently bright episodes of hardening should have been detected over ~ 4 years of the *Swift* mission.

Our systematic search of the episodes of ‘high-confidence’ hardening of *Swift* GRB spectra has revealed that if the time binning of the GRBs is chosen in a way similar to that adopted for the analysis of BATSE time-resolved GRB spectra, only two GRBs have sufficiently bright and long episode of spectral hardening. Remarkably, these are the two highest fluence GRBs in the *Swift* GRB sample. The spectral hardening is observed in five time intervals in total, compared to ~ 30 expected from the re-scaling of BATSE data. We have demonstrated that the slight discrepancy between the real and the simulated data disappears if one takes into account the fact that the errors of measurement of the photon index in the simulated data are underestimated, because the simulation procedure ignores the possibility that GRB could be detected in the partially coded field of view.

Relaxing the requirement on the S/N imposed for the time binning of the GRB light curves for the time-resolved spectral analysis, we have found that, in fact, more GRBs in the *Swift* GRB sample possess the intervals of hardening beyond $\Gamma = 2/3$. The light curves of these bursts and the evolution of the photon indices over the burst duration are shown in Fig. 6. Given the very low statistics of the observations of ‘high-confidence’ hard spectra in the *Swift* GRB sample, the only firm conclusion which can be drawn at the moment is that *Swift* data confirm the fact of *existence* of the episodes of spectral hardening of the GRB prompt emission beyond the ‘synchrotron deathline’.

To summarize the results of our investigation, we find that statistics of detections of the episodes of spectral hardening of the GRB spectra beyond $\Gamma = 2/3$ in *Swift* are consistent with previous BATSE result on the existence of a significant fraction of time-resolved GRB spectra ‘beyond the synchrotron deathline’.

The existence of the GRB spectra ‘beyond the synchrotron deathline’ rules out a model in which prompt γ -ray emission of GRB is the optically thin synchrotron emission from a population of electrons moving in a random magnetic field (the model most commonly adopted within the ‘relativistic fireball’ approach for the modelling of prompt emission) (Zhang & Mészáros 2004; Piran 2005). Several possible solutions of the problem of the ‘too hard’ photon indices are available, such as the synchrotron/curvature/‘jitter’ emission mechanism by electrons is moving at small pitch angles $\theta \sim \gamma^{-1}$ in magnetic field (Epstein 1973; Medvedev 2000; Lloyd-Ronning & Petrosian 2002; Baring & Braby 2004) or optically thick synchrotron mechanism with the synchrotron self-absorption energy reaching ~ 100 keV (Lloyd & Petrosian 2000) or the inverse Compton scattering mechanism (Shemi 1994; Shaviv & Dar 1995; Lazatti

et al. 2000; Panaitescu & Mészáros 2000; Dar & De Rújula 2004; Kumar & McMahon 2008; Piran et al. 2009).

ACKNOWLEDGMENTS

We would like to thank T. Courvoisier and V. Beckmann for the useful discussions of the subject and for the comments on the manuscript.

REFERENCES

- Akerlof C. et al., 1999, *Nat*, 398, 400
 Band D. L. et al., 1993, *ApJ*, 413, 281
 Baring M. G., Braby M. L., 2004, *ApJ*, 613, 460
 Barraud C. et al., 2003, *A&A*, 400, 1021
 Barthelmy S. et al., 2005, *Nat*, 438, 994
 Bhat P. N., Fishman G. J., Meegan C. A., Wilson R. B., Brock M. N., Paciesas W. S., 1992, *Nat*, 359, 217
 Costa E. et al., 1997, *Nat*, 387, 783
 Dar A., De Rújula A., 2004, *Phys. Rep.*, 405, 203
 Epstein R. I., 1973, *ApJ*, 183, 593
 Fenimore E. E., Epstein R. I., Ho C. H., 1993, *A&AS*, 97, 59
 Fox D. B. et al., 2005, *Nat*, 437, 845
 Frail D. A., Kulkarni S. R., Nicastro L., Feroci M., Taylor G. B., 1997, *Nat*, 389, 261
 Galama T. J. et al., 1998, *Nat*, 395, 670
 Gehrels N. et al., 2004, *ApJ*, 611, 1005
 Gehrels N. et al., 2005, *Nat*, 437, 851
 Hjorth J. et al., 2005, *Nat*, 437, 859
 Kaneko Y., Preece R. D., Briggs M. S., Paciesas W. S., Meegan C. A., Band D. L., 2006, *ApJS*, 166, 298
 Katz J. I., 1994, *ApJ*, 432, L107
 Kumar P., McMahon E., 2008, *MNRAS*, 384, 33
 Lazatti D., Ghisellini G., Celotti A., Rees M., *ApJ*, 2000, L17
 Lloyd N. M., Petrosian V., 2000, *ApJ*, 543, 722
 Lloyd-Ronning N. M., Petrosian V., 2002, *ApJ*, 565, 182
 Medvedev M. V., 2000, *ApJ*, 540, 704
 Panaitescu A., Mészáros P., 2000, *ApJ*, 544, L17
 Piran T., 2005, *Rev. Mod. Phys.*, 76, 1143
 Piran T., Sari R., Zou Y.-C., 2009, *MNRAS*, 393, 1107 (arXiv:0807.3954)
 Preece R. D., Pendleton G. N., Briggs M. S., Mallozzi R. S., Paciesas W. S., Band D. L., Matteson J. L., Meegan C. A., 1998a, *ApJ*, 496, 849
 Preece R. D., Briggs M. S., Mallozzi R. S., Pendleton G. N., Paciesas W. S., Band D. L., 1998b, *ApJ*, 506, L23
 Preece R. D., Briggs M. S., Mallozzi R. S., Pendleton G. N., Paciesas W. S., Band D. L., 2000, *ApJS*, 126, 19
 Racusin J. L. et al., 2008, *Nat*, 455, 183
 Roming P. W. A. et al., 2006, *ApJ*, 651, 985 (astro-ph/0605005)
 Savchenko V., Neronov A., Couvoisier T. J.-L., 2009, *A&A*, submitted
 Shaviv N. J., Dar A., 1995, *MNRAS*, 277, 287
 Shemi A., 1994, *MNRAS*, 269, 1112
 Stanek K. Z. et al., 2003, *ApJ*, 591, 17
 Tavani M., 1995, *Ap&SS*, 231, 181
 van Paradijs J. et al., 1997, *Nat*, 386, 686
 Vestrand W. T. et al., 2005, *Nat*, 435, 178
 Vestrand W. T. et al., 2006, *Nat*, 442, 172
 Walker K. C., Schaefer B. E., Fenimore E. E., 2000, *ApJ*, 537, 264
 Woods E., Loeb A., 1995, *ApJ*, 383, 292
 Zhang B., Mészáros P., 2004, *Int. J. Mod. Phys. A*, 19, 2385
 Zou Y.-C., Piran T., Sari R., 2008, preprint (arXiv0812.0318)

This paper has been typeset from a \LaTeX file prepared by the author.